Electronic Supplementary Information

Raman and infrared spectroscopy differentiate senescent from proliferating cells in a human dermal fibroblast 3D skin model

Katharina Eberhardt,[a,b] Christian Matthäus,[a,b] Doreen Winter,[c] Cornelia Wiegand,[c] Uta-Christina Hipler,[c] Stephan Diekmann[d] and Jürgen Popp[a,b]

[a] Leibniz Institute of Photonic Technology Jena, Albert-Einstein-Str. 9, 07745 Jena (Germany)

[b] Institute for Physical Chemistry and Abbe Center of Photonics, Friedrich Schiller University Jena, Helmholtzweg 4, 07743 Jena (Germany)

[c] University Hospital Jena, Department of Dermatology, Erfurter Str. 35, 07740 Jena (Germany)

[d] Leibniz Institute on Aging – Fritz Lipmann Institute, Department of Molecular Biology, Beutenbergstr. 11, 07745 Jena (Germany)

Content

1. Spheroid images

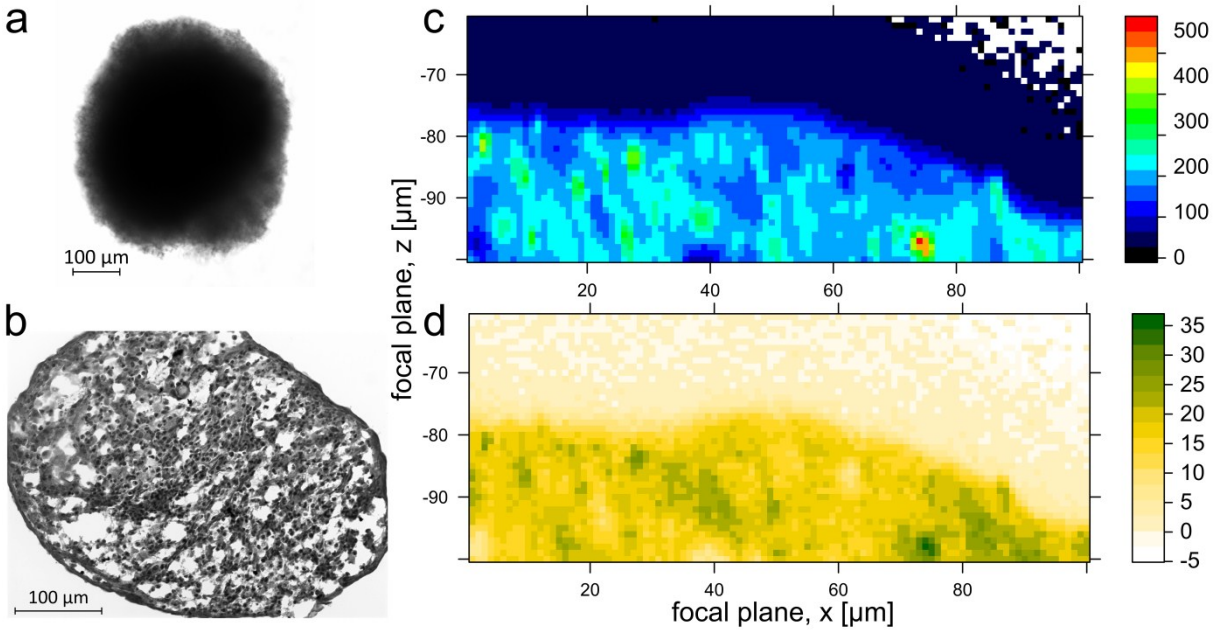

Fig. S1: Formaldehyde-fixed spheroid (a) consisting of aggregated BJ fibroblast cells (PD 28). Hematoxylin and eosin staining (b) of a cryotome cut displays nuclei (dark and round shape) within a spheroid formed of PD 28 (3 x 10^4 cells/well), after 1 day encapsulated with PD 56 cells (5 x 10^3 cells/well). Intensity-related Raman image depth scan (c) of the encapsulated spheroid using intensities of the C-H-stretching vibrations (from 2800 to 3020 cm^{-1}). False-color map (d) of nucleic acid distribution (using DNA intensity-related bands at 722, 786, 1094, 1242, 1478 and 1578 cm^{-1}) shows nuclei (dark green) within the spheroid (yellow). Scale Bar (a, b) is 100 µm.

2. Spheroid clustering

The Raman data were subjected to a hierarchical cluster analysis (HCA, using Ward's method [1]) as routinely applied for cancerous tissues and cancer cell lines.[2] Within the image, the outer area with scattered cell fragments was removed. The spectral information of the obtained image was grouped according to their similarities, to contrast cellular locations within the spheroid. Five clusters were selected to visualize the layers close to the spheroid surface. The statistical distances between these selected groups (nuclei, cytoplasm (arbitrarily selected twice), lipid-richer interspace between cells, spheroid surface) were displayed (Fig. S2a). The plot indicates that the

Raman data recognize the selected cellular compartments as biochemically similar, and each one as different from other compartments. Based on these data, false color cluster maps were generated. In the false color spheroid image (Fig. S2b), structures corresponding to single cells and their nuclei could be identified. The corresponding Raman spectra (Fig. S2c) showed weak group specific differences which were sufficient to distinguish the groups in the HCA plot.

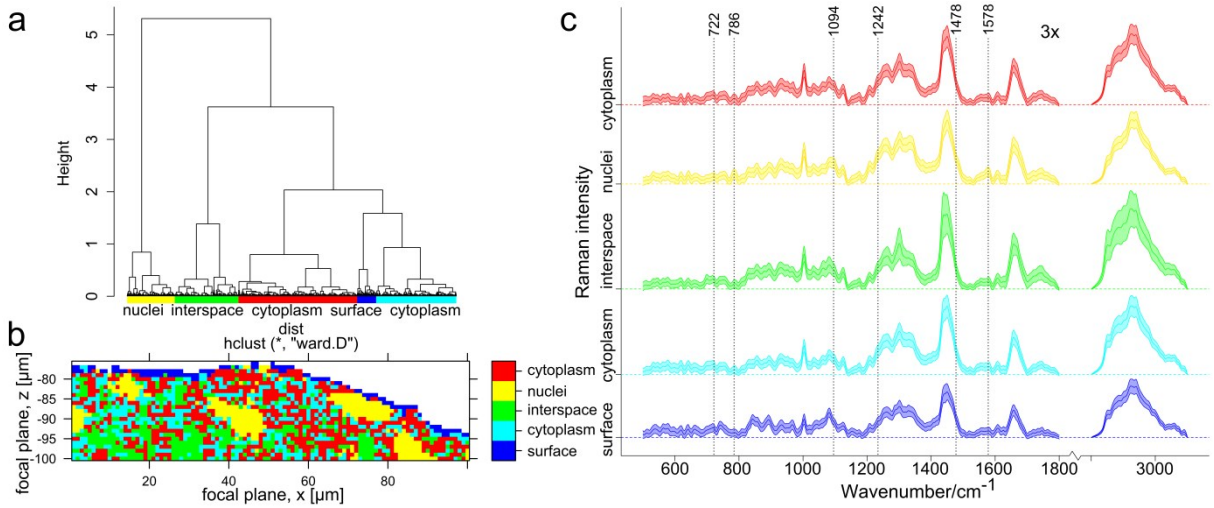

Fig. S2: Raman spectra-related hierarchical clustering of a depth scan into the spheroid. Dendrogram (a) of 5 selected clusters ("height"), depicted with possible cell regions. These indicated spectral similarities. Cluster memberships are plotted in a false-color cluster map (b). Calculated cluster mean spectra +/- SD of all Raman spectra (c). Depicted Raman bands indicated the mentioned DNA-related bands. The low wavenumber region from 500 to 1800 cm^{-1} of the Raman spectra is three-fold increased.

3. Band assignments of Raman and FTIR data

Table S1: Band assignments of Raman (left) and FTIR spectra (right), as suggested in the literature.[3, 4]

Raman wavenumber (cm^{-1})	Band assignments	Biomolecular classifications	Infrared wavenumber (cm^{-1})	Band assignments	Biomolecular classifications
2800 - 3020	ν(CH, CH_2 & CH_3) sym. & asym.	lipids & proteins	**2800 - 3100**	ν(CH_2 & CH_3) sym. & asym.	lipids, proteins
1620 - 1654	amide I, ν(C=C & C=O), α-helix	proteins, lipids	**1748**	ν(C=O)	lipids
1572	guanine, adenine ring breathing	nucleic acids, DNA, RNA	**1732**	ν(C=O)	lipids
1440 - 1452	δ_s(CH_2 & CH_3)	lipids, proteins	**1668 - 1672**	pleated sheets & β-structure	proteins
1200- 1340	amide III, δ(CH_2), ν(CN) & δ(NH), ring breathing	proteins, collagen, lipids, DNA, RNA	**1600 - 1700**	amide I, β-structure	proteins
1176	ν(CH) bending; cytosine, guanine	proteins; DNA, RNA	**1500 -1600**	amide II, α-helix, β-structure	proteins
1060	ν(PO_2^-), ν(C-C & C-O)	DNA, RNA, lipids	**~1520**	tyrosine	proteins
1004	ring breathing	phenylalanine	**1448**	ν(CH_3) asym. bending, δ(CH_3)	proteins, collagen
986	ν(C-C), β-structure, ν(=CH) bending	proteins, collagen, lipids	**1396**	ν(C=0) sym., ν(C-N)	lipids, collagen
928	ν(C-C)	proteins, collagen	**1244**	amide III, ν(C-N), ν(C-C), ν(P=O) asym.	collagen, DNA, RNA
~880	ring breathing, ν(C-C)	nucleic acid, DNA, RNA, tryptophan, collagen	**1108 - 1112**	ν(C-C & C-O), ring vibration	carbohydrates
~785 & ~795	pyrimidine & uracile ring breathing	DNA, RNA	**1032 & 1080**	ν(C-O)	nucleic acid
~725	ring breathing	DNA, RNA	**1024**	ring deformation	glycogen
			900 - 1200	ν(P=O) sym., C-O-C & C-O ring vibrations, C-O-P, P-O-P	nucleic acid; carbohydrates

ν - stretching; δ - deformation; δ_s - scissoring; γ_t - twisting; γ_w - wagging;
sym. - symmetric; asym. - asymmetric.

4. Difference spectra of Raman and FTIR data

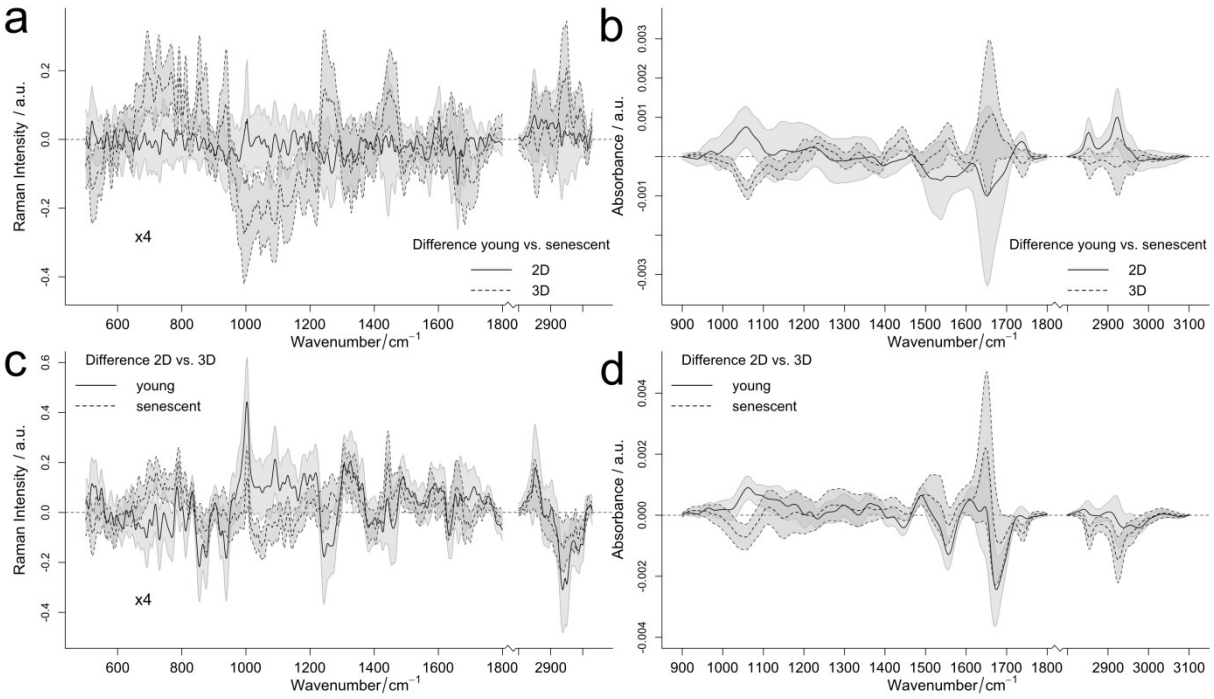

Fig. S3: Calculated mean and standard deviation (gray shading) of difference spectra of Raman (a, c) and FTIR data (b, d) of all young versus all senescent cells (a, b) cultivated within 2D (HDF, solid line) or 3D models (FDM, dashed line) and of all 2D versus 3D cultivated cells (c, d) within the young (solid line) or the senescent (dashed line) group. For better visualization of the Raman difference spectra (a, c), the low wavenumber region from 500 to 1800 cm^{-1} was plotted four-fold enhanced.

REFERENCES

1. J. H. Ward, *Journal of the American Statistical Association*, 1963, **58**, 236-244.
2. M. Diem, M. Miljković, B. Bird, T. Chernenko, J. Schubert, E. Marcsisin, A. Mazur, E. Kingston, E. Zuser, K. Papamarkakis and N. Laver, *Spectroscopy: An International Journal*, 2012, **27**, 463-496.
3. Z. Movasaghi, S. Rehman and I. U. Rehman, *Applied Spectroscopy Reviews*, 2007, **42**, 493-541.
4. D. Naumann, *Applied Spectroscopy Reviews*, 2001, **36**, 239-298.